Next-generation sequencing study of inflammatory spindle cell lesions focused on receptor tyrosine kinase gene rearrangements most frequently occurring in inflammatory myofibroblastic tumor

Krzysztof Siemion[1,2,A–F], Joanna Kiśluk[3,B,D,E], Natalia Wasilewska[3,B,D,E], Joanna Reszec-Gielażyn[1,D–F], Anna Korzyńska[2,D–F], Tomasz Łysoń[4,E,F], Zenon Mariak[4,E,F]

[1] Department of Medical Pathomorphology, Medical University of Bialystok, Poland
[2] Laboratory of Processing and Analysis of Microscopic Images, Nalecz Institute of Biocybernetics and Biomedical Engineering, Polish Academy of Sciences, Warsaw, Poland
[3] Department of Clinical Molecular Biology, Medical University of Bialystok, Poland
[4] Department of Neurosurgery, Medical University of Bialystok, Poland

A – research concept and design; B – collection and/or assembly of data; C – data analysis and interpretation; D – writing the article; E – critical revision of the article; F – final approval of the article

Advances in Clinical and Experimental Medicine, ISSN 1899–5276 (print), ISSN 2451–2680 (online) *Adv Clin Exp Med*. 2025;34(12):2119–2135

Address for correspondence
Krzysztof Siemion
E-mail: krzysztof.siemion@ibib.waw.pl

Funding sources
The study was financed from funds of the Medical University of Bialystok (grants No. SUB/1/DN/21/002/1194 and No. SUB/1/DN/22/002/1155) and Nalecz Institute of Biocybernetics and Biomedical Engineering Polish Academy of Sciences (grant No. FBW/3.1/23).

Conflict of interest
None declared

Received on January 28, 2024
Reviewed on December 10, 2024
Accepted on March 19, 2025

Published online on July 31, 2025

Cite as
Siemion K, Kiśluk J, Wasilewska N, et al. Next-generation sequencing study of inflammatory spindle cell lesions focused on receptor tyrosine kinase gene rearrangements most frequently occurring in inflammatory myofibroblastic tumor. *Adv Clin Exp Med*. 2025;34(12):2119–2135. doi:10.17219/acem/203097

DOI
10.17219/acem/203097

Abstract

Background. A group of inflammatory spindle cell lesions (ISCLs) includes many nosological entities with a common histological image consisting of spindle-shaped cells and inflammatory infiltrate. Diverse diseases indicate different prognoses that can be difficult to predict. The most well-known neoplasm from the group is an inflammatory myofibroblastic tumor (IMT) that harbors tyrosine kinase gene rearrangement frequently affecting *ALK*, *ROS*1, *RET*, *PDGFRB*, *NTRK*, and *IGF1R* genes. In contrast, a reactive mass-forming lesion is regarded as an inflammatory pseudotumor (IPT).

Objectives. This study aimed to: 1) investigate the accuracy of the primary diagnosis of IMT and IPT with the diagnostics using extended analysis of clinical data, re-evaluation of histopathological slides and next-generation sequencing (NGS); and 2) to establish prognostic and diagnostic factors.

Materials and methods. Finally, 46 cases of ISCLs were retrieved. The authors revised diagnoses and performed NGS based on ribonucleic acids isolated from selected paraffin blocks. Clinical and paraclinical data were also collected. The final diagnoses were made as a result of available information integration.

Results. The sequencing confirmed 4 IMTs and detected 4 fusion gene types – *EML4-ALK*, *RANBP2-ALK*, and *ETV6-NTRK3*. Additionally, 1 afunctional EGFR-PPARGC1A rearrangement was found in gastric inflammatory fibroid polyp. A subset of reactive lesions also contained some mutations, which is consistent with actual knowledge. Neoplasms with ganglion-like cells, nuclear atypia and increased mitotic activity gave local recurrences. A higher percentage of necrosis indicated IMTs and patients who died in the analyzed period. No relation between genetic alterations and relapse was found.

Conclusions. A final diagnosis can be made based on all clinical and paraclinical data. The prognosis after the treatment is dependent on the pathological diagnosis, disease location and resection completeness, presence of ganglion-like cells, nuclear atypia, mitotic index, and necrosis. Not only neoplastic but also reactive lesions can recur. The presence of gene rearrangements and necrosis can have diagnostic value.

Key words: next-generation sequencing, receptor tyrosine kinase, inflammatory myofibroblastic tumors, inflammatory pseudotumors, inflammatory spindle cell lesions

Highlights

- Inflammatory spindle cell lesions (ISCLs) feature spindle cells mixed with inflammatory infiltrates – hallmark morphology for this rare entity.
- ISCL spectrum ranges from neoplastic inflammatory myofibroblastic tumors (IMTs) to reactive inflammatory pseudotumors (IPTs).
- Neoplastic and reactive ISCLs alike can exhibit aggressive histology, oncogenic mutations and clonal genetic changes.
- Tyrosine receptor kinase gene rearrangement testing (ALK, ROS1, NTRK) is mandatory for a definitive IMT diagnosis.
- Pathology reports should list prognostic and diagnostic markers – ganglion-like cells, cytologic atypia, mitotic index, necrosis, and gene rearrangements.

Background

Inflammatory spindle cell lesions (ISCLs) represent a histologically defined group of disorders. Microscopically, they are characterized by the presence of spindle-shaped cells interspersed with a dense inflammatory infiltrate (Fig. 1). This group is heterogeneous in nature, encompassing a range of distinct pathological entities.[1–4] Initially, ISCLs were divided into 2 subgroups: 1) a neoplastic lesion – an inflammatory myofibroblastic tumor (IMT); and 2) a reactive lesion – an inflammatory pseudotumor (IPT).[1] Subsequently, the group was gradually expanded.[3,5–18] Any secondary inflamed spindle cell neoplasm may be included in this group. However, establishing an accurate diagnosis can be challenging.[19]

Inflammatory spindle cell lesions may occur in any region of the human body, with symptoms and signs depending on the location.[3] Radiological imaging is often heterogeneous and nonspecific.[20] Correlation of histological features, molecular genetic testing, clinical history, and radiological data is essential for accurate diagnosis.

Inflammatory myofibroblastic tumors are intermediate-grade neoplasms characterized by a relatively high recurrence rate and low metastatic potential. Under a light

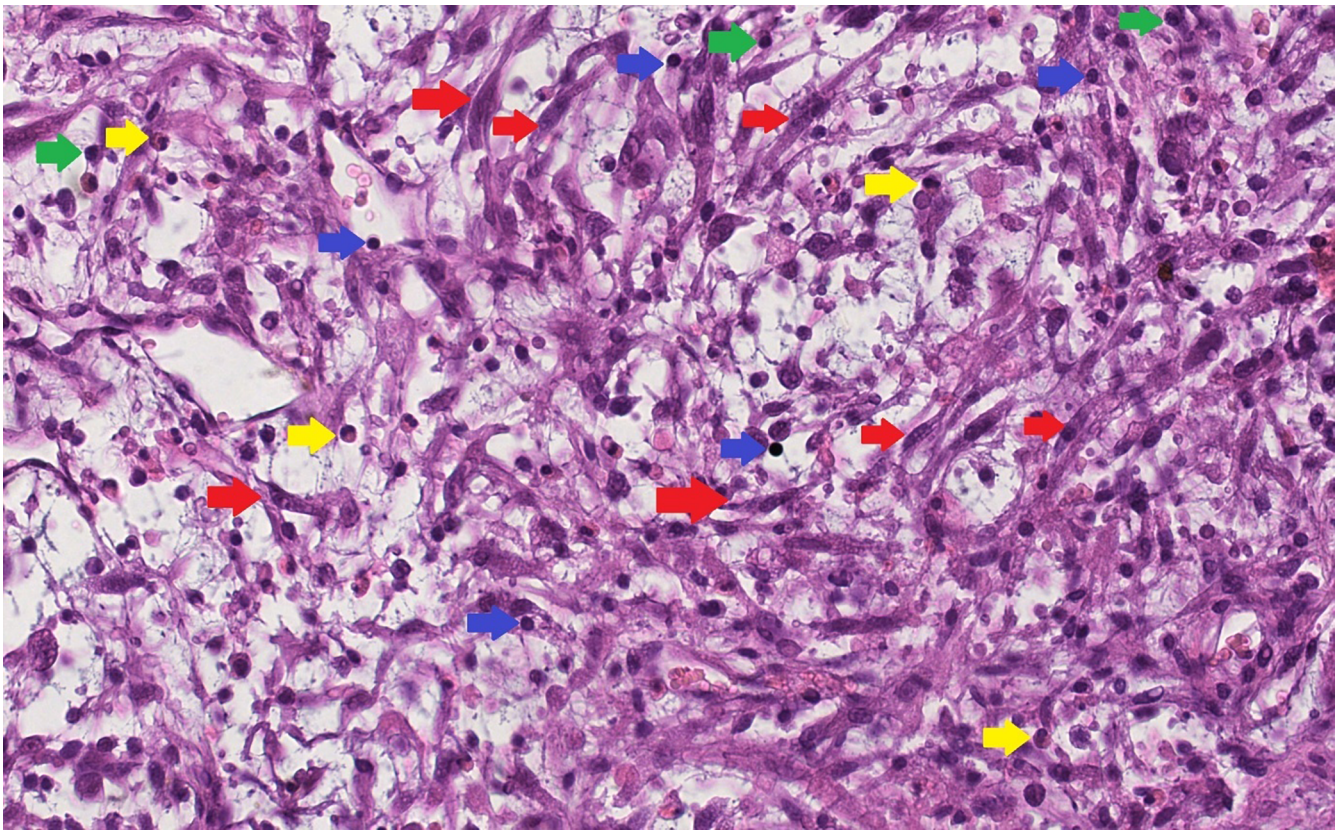

Fig. 1. Histopathological image of an inflammatory spindle cell lesion is composed of spindle cells (red arrows) and inflammatory infiltrate. Blue arrows: lymphocytes, green arrows: plasma cells, yellow arrows: eosinophils

microscope, 3 major histopathological patterns can be distinguished: classical, hypocellular and hypercellular. A hypercellular pattern, high mitotic activity, presence of myxoid stroma, ganglion-like cells, multinucleated giant cells, necrosis, lymphovascular invasion, and infiltrative growth are considered adverse prognostic factors.[3,21] Approximately 50–60% of IMTs harbor *ALK* gene rearrangements. Other gene fusions – such as *ROS1, PDGFRB, RET, NTRK1/3*, and *IGF1R* – occur less frequently. Prior to the identification of these driver fusion genes, the terms IMT and IPT were sometimes used interchangeably by clinicians.[3]

Objectives

The aim of the study was to: 1) investigate the accuracy of primary diagnoses of IMT and IPT by incorporating extended clinical data analysis, re-evaluation of histopathological slides and next-generation sequencing (NGS); 2) determine whether pathological diagnoses, disease location, histological features, and genetic changes influence local recurrence of ISCLs.

Materials and methods

Participants

Eighty-five cases of ISCLs, initially diagnosed as IMT or IPT, were retrieved from the Department of Medical Pathomorphology, Medical University of Bialystok (Poland) database. After excluding 39 cases, 46 patients were included in the study (22 men and 24 women; most common lesion locations: abdomen and orbit). Based on the final histopathological diagnoses, the cases were classified into 2 groups: neoplastic (n = 24) and reactive (n = 22). Clinical and paraclinical data collected before and after diagnosis were analyzed for both groups.

Design and settings

The study was approved by Guidelines for Good Clinical Practice by the Bioethical Committee at the Medical University of Bialystok (approval No. APK.002.339.2020). First, archival formalin-fixed paraffin-embedded (FFPE) blocks were prepared using the Leica TP1020 tissue processor (Leica Camera AG, Wetzlar, Germany) and the HistoCore Arcadia H + C embedding system (Leica Camera AG) before the study. At this stage, standard reagents, including 10% buffered neutral formalin, xylene (isomeric mixture), ethanol, and paraffin wax, were used. Then, using the HistoCore AUTOCUT microtome (Leica Camera AG), 4–5 µm-thick sections were prepared and placed on SuperFrost Plus base glasses (Thermo Fisher Scientific, Waltham, USA). Hematoxylin and eosin (H&E) staining was performed using the ST5010 Autostainer XL (Leica Camera AG). Finally, histopathological slides were covered using CV5030 Glass Coverslipper (Leica Camera AG).

The initial evaluation of H&E-stained histopathological slides was performed by the 1st pathologist (K.S.) using a light microscope (Olympus BX43; Olympus Corp., Tokyo, Japan). A second opinion was provided for each case by the 2nd pathologist (J.R.G.). Final assessments were based on consensus between the 2 specialists. The histopathological evaluation included the following criteria:

– overall pattern (classical, hypocellular or hypercellular);
– degree of nuclear atypia, assessed according to the criteria proposed by Weir et al.[22];
– percentage of necrosis;
– mitotic index, defined as the number of mitoses per 10 high-power fields (HPF);
– intensity of the inflammatory infiltrate, graded according to the method presented by Klintrup et al.[23];
– predominant type of inflammatory cells within the infiltrate;
– presence of ganglion-like cells, angioinvasion and perineural invasion.

Two pathology specialists reviewed all cases and selected 46 for the NGS procedure. Genomic RNA was extracted from the macrodissected FFPE material using the AllPrep DNA/RNA FFPE Kit (Qiagen, Hilden, Germany). Quantity and quality of isolated RNA were determined using the NanoDrop 1000 UV Spectrophotometer (Thermo Fisher Scientific) and Qubit Fluorometer (Thermo Fisher Scientific).

Sample analysis was performed by NGS technology with the Archer® Fusion Plex® Lung Kit v. PI028.1 (ArcherDX, Inc, Boulder, USA) on the Illumina MiSeq platform. The NGS-based targeted sequencing assay allows detection of known and novel gene fusions, single nucleotide variations (SNVs), insertion/deletion polymorphism (indels), splicing, and gene expression. The kit contains 163 GSPs targeting 14 genes. The unique molecular on-target is above 93%. The assay targets are presented in Table 1. The recommended number of reads for all targets was 500,000. Data were analyzed using the Lung Target Region File and vendor-supplied software (Archer Analysis v. 6.2.7; Integrated DNA Technologies Inc.). The limit of detection (LoD) was defined as a minimum of 5 reads with at least 3 unique sequencing start sites spanning the breakpoint regions. The read length was paired-end, with a cut-off of 5% for variant allele frequency (VAF). The median coverage for all samples was 1,350.

Criteria

Following the analysis of clinical and paraclinical data, histopathological slide assessments and NGS results, the final diagnoses were established by 2 pathologists based on the World Health Organization (WHO) soft

Table 1. Next-generation sequencing target genes

Gene	Exons
ALK	NM_004304 exon 22, 23, 25 mutations
	NM_004304 exon 2, 4, 6, 10, 16, 17, 18, 19, 20, 21, 22, 23, 26 fusions 5′
BRAF	NM_004333 exon 15 mutation (V600)
	NM_004333 exon 2, 7, 8, 9, 10, 11, 12, 15, 16 fusion 5′
	NM_004333 exon 1, 3, 7, 8, 10, 13 fusion 3′
EGFR	NM_005228 exon 18, 19, 20, 21 mutations
	NM_005228 exon 7, 8, 9, 16, 19, 20, fusion 5′
	NM_005228 8 exon 2–7 skipping (EGFRvIII) 5′
	NM_005228 exon 1, 24, 25 fusion 3′
	NM_005228 1 exon 2–7 skipping (EGFRvIII) 3′
FGFR1	NM_015850 exon 2, 3, 4, 5, 6, 7, 8, 9, 10, 11, 17 fusions 5′
	NM_015850 exon 12, 17 fusion 3′
FGFR2	NM_000141 exon 2, 5, 7, 8, 9, 10 fusion 5′
	NM_000141 16, 17 fusion 3′
FGFR3	NM_000142 exon 3, 5, 8, 9, 10 fusion 5′
	NM_000142 exon 16, 17, 18 fusion 3′
KRAS	NM_004985 exon 2, 3 mutation
MET	NM_000245 exon 2, 4, 5, 6, 13, 14, 15, 16, 17, 21 fusion 5′
	NM_000245 15 exon 14 skipping 5′
	NM_000245 exon 2, 13 fusion 3′
	NM_000245 13 exon 14 skipping 3′
NRG1	NM_013957 exon 1, 8 fusion 5′
	NM_004495 exon 1, 2, 3, 4, 6 fusion 5′
	NM_013962 exon 1 fusion 3′
NTRK1	NM_002529 exon 2, 4, 6, 8, 10, 11, 12, 13 fusion 5′
NTRK2	NM_006180 exon 5, 7, 9, 11, 12, 13, 14, 15, 16, 17 fusion 5′
NTRK3	NM_002530 exon 4, 7, 10, 12, 13, 14, 15, 16 fusion 5′
	NM_001007156 exon 15 fusion 5′
	NM_002530 exon 13, 14, 15 fusion 3′
RET	NM_020630 exon 15,16 mutation
	NM_020630 exon 2, 4, 6, 8, 9, 10, 11, 12, 13, 14 fusion 5′
ROS1	NM_002944 exon 38 mutation
	NM_002944 exon 2, 4, 7, 31, 32, 33, 34, 35, 36, 37 fusion 5′

ALK – anaplastic lymphoma kinase; BRAF – B-type rapidly accelerated fibrosarcoma; EGFR – epidermal growth factor receptor; FGFR – fibroblast growth factor receptor; KRAS – Kirsten rat sarcoma; MET – mesenchymal-to-epithelial transition factor; NRG1 – neuregulin 1; NTRK – neurotrophic tyrosine receptor kinase; RET – rearranged during transfection; ROS1 – v-ras avian UR2 sarcoma virus oncogene homolog 1.

tissue tumor classification criteria[24] (Fig. 2). The inclusion criteria were: 1) primary histopathological diagnosis of IMT or IPT; 2) presence of FFPE blocks; 3) spindle cell morphology with inflammatory infiltrate resembling IMT; and 4) RNA integrity number (RIN) with a minimum value of 2. Cases were excluded if FFPE material was unavailable, if histopathological features differed from the study criteria, or if the RNA integrity number (RIN) was below 2.

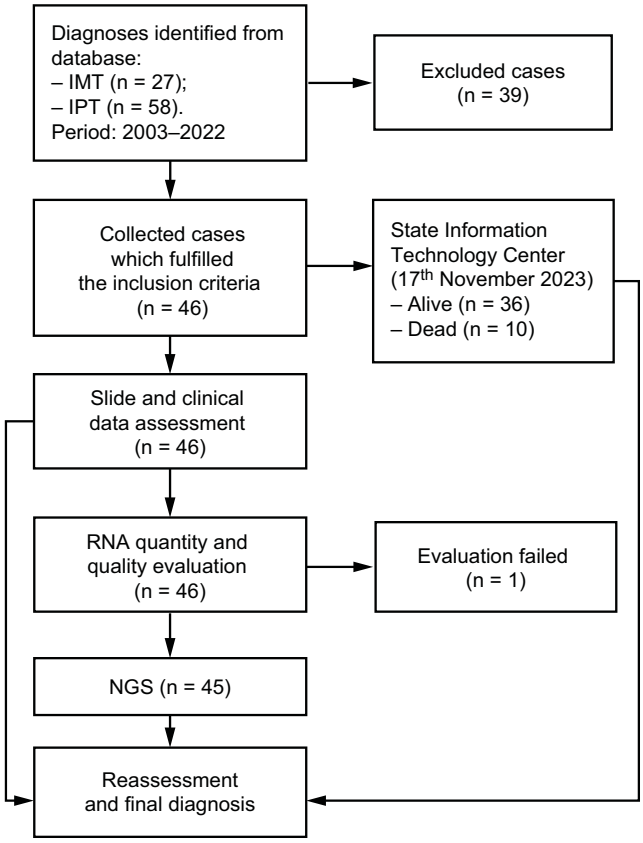

Fig. 2. Diagram depicting the data collection and work schedule

FFPE – formalin-fixed paraffin-embedded; IMT – inflammatory myofibroblastic tumor; IPT – inflammatory pseudotumor.

Statistical analyses

The statistical parameter formulas and definitions used for diagnostic verification are outlined in Fig. 3. Dichotomous division was used at each stage of the analysis, e.g., neoplasms compared to other diseases, IMTs compared to other ISCLs, recurrent compared to non-recurrent cases, and patients who died compared to those who survived. To assess the impact of the dichotomous classification, odds ratios (ORs) and 95% confidence intervals (95% CIs) for the 2 proportions were calculated using the method described by Tenny et al.[25] These statistical parameters were selected because they effectively quantify the strength of association between the 2 groups (with and without events) in retrospective studies.[25] Probability values (p-values) were calculated using the MedCalc online calculator (https://www.medcalc.org).

All numerical data (e.g., necrosis percentage, mitotic index) obtained through light microscopy represented subjective assessments by the pathologists. While these should be considered continuous variables, they could not be assumed to follow a normal distribution. The data obtained using NGS should be treated similarly. At each stage of the analysis, values were categorized into 1 of 2 groups; therefore, a nonparametric test was selected to account for

a

Parameter	
sensitivity	$\frac{TP}{TP+FN}$
specificity	$\frac{TN}{TN+FP}$
accuracy	$\frac{TP+TN}{TP+FP+TN+FN}$
precision	$\frac{TP}{TP+FP}$
F1 score	$\frac{2TP}{2TP+FP+FN}$

b

neoplasm diagnosis correctness	Primary diagnosis	Final diagnosis
TP	neoplasm	neoplasm
TN	other diseases	other diseases
FN	other diseases	neoplasm
FP	neoplasm	other diseases

c

IMT diagnosis correctness	Primary diagnosis	Final diagnosis
TP	IMT	IMT
TN	other diseases	other diseases
FN	other diseases	IMT
FP	IMT	other diseases

Fig. 3. A. Statistical parameter formulas; B. Definitions used during verification of neoplasm diagnosis correctness; C. Definitions used during verification of inflammatory myofibroblastic tumor diagnosis correctness

FN – false negative; FP – false positive; IMT – inflammatory myofibroblastic tumor; TN – true negative; TP – true positive.

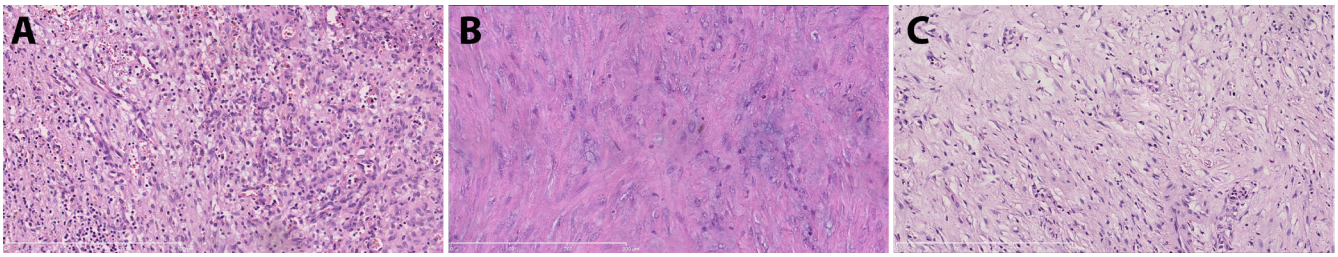

Fig. 4. Tissue pattern. A. Classical (case 4); B. Hypercellular (case 5); C. Hypocellular (case 2). Hematoxylin and eosin (H&E) slides, ×200 magnification

the data distribution. A two-tailed Mann–Whitney U test was conducted at a 5% significance level using the Statistics Kingdom online calculator (https://www.statskingdom.com). Outlier values were included in the analysis.

Results

Histopathological assessment

The predominant tissue patterns were classical (41.3%), mixed (30.4%) and hypocellular (17.4%) (Fig. 4). Nuclear atypia was observed in 17 cases (37%), mostly mild, while 3 cases (6.5%) contained ganglion-like cells. Necrosis was present in 26 cases (56.5%). Approximately ¾ of the lesions showed no mitoses. Chronic inflammatory infiltrates, primarily composed of lymphocytes and plasma cells, dominated among the cases. Angiovascular and perineural invasion were not observed.

The ORs for the presence of atypia and mitoses in neoplastic lesions compared to reactive lesions were statistically significant at the 95% confidence level: OR = 7.48 (95% CI: 1.74–32.17, p = 0.007) and OR = 7.14 (95% CI: 1.35–37.75, p = 0.021), respectively. These values were calculated using the method described by Tenny et al.[25]

The estimated necrosis percentage in IMTs (cases 1, 2, 3, 4, and 46) compared to other ISCLs was evaluated using the Mann–Whitney U test (U = 162.5, p = 0.028). A statistically significant difference was observed, with the 1st group exhibiting a mean value of 34.2% compared to 11.9% in the 2nd group, at the 95% CI (Fig. 5). Based on histopathological features and clinical data, 46 cases were qualified for molecular diagnostics.

Molecular diagnostics

Gene fusions

One sample (case 46) failed RNA quality and quantity control because the RIN value was below 2. Fusion genes were identified in 5 cases. Among them, 4 cases were ultimately diagnosed as IMTs due to the presence of tyrosine kinase rearrangements. Cases 1 and 2 presented an *EML4-ALK* fusion, while case 3 displayed a *RANBP2-ALK* fusion, which led to the diagnosis of epithelioid inflammatory myofibroblastic sarcoma (EIMS) – a more aggressive

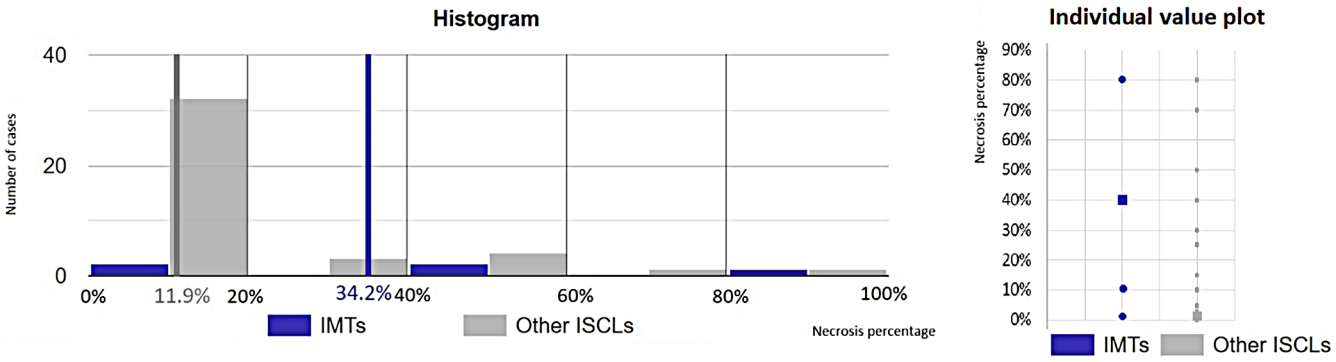

Fig. 5. Histogram (left) depicts the distribution of necrosis percentage values among inflammatory myofibroblastic tumors (IMTs; blue) and other inflammatory spindle cell lesions (ISCLs; grey). The arithmetic mean values are marked with vertical lines. Axes: abscissa – necrosis percentage intervals in the histopathological slides: [0–20%], [20–40%), [40–60%), [60–80%), and [80–100%]; ordinate – number of cases. Individual value plot (right) shows a dot for the actual value of each observation in both groups. The median values are marked with squares. Axes: abscissa – groups of cases (blue: IMTs, grey: other ISCLs); ordinate – necrosis percentage

Table 2. Collective description of fusion genes diagnosed in neoplasms during the study

Case number	Diagnosis	Pattern	Atypia	Necrosis	Inflammatory infiltrate intensity	Dominating inflammatory cells	IHC	Fusion gene	Breakpoints	Recurrence	Observation period
1	IMT of the external nose	C	mild	10%	severe	histiocytes	(+): SMA; (–) S100	EML4-ALK	chr2:42522656 (exon 13) chr2:29446394 (exon 18)	1 year	7 years
2	hepatic IMT	C/↓	none	1%	severe	neutrophils	(+): vim, SMA, CD 99; (–): CK,CD 10, CD31, CD34; Ki67: low	EML4-ALK	chr2:42492091 (exon 6) chr2:29446394 (exon 18)	none	8 years
3	EIMS of the left sphenoid sinus	C	moderate	40%	moderate	lymphocytes, plasma cells, neutrophils	(+): SMA; ALK (focally); (–): CK, CD34; Ki67: 10%	RANBP2-ALK	chr2:110449532 (intron 24) chr2:29443649 (exon 23)	none	7 years
4	IMT of the right orbit	C	mild	80%	moderate	lymphocytes, plasma cells, neutrophils	not performed	ETV6-NTRK3	chr12:12022903 (exon 5) chr15:88483984 (exon 15)	none	1 year
5	gastric IFP	↑	mild	1%	mild	eosinophils	(+): CD34, SMA; (–): desmin, H-caldesmon, ALK, CK, CD117, DOG1	EGFR-PPARGC1A	chr7:55087048 (exon 1) chr4:23926271 (exon 2)	none	4 years

↓ – hypocellular; ↑ – hypercellular; (–) – negative; (+) – positive; ALK – anaplastic lymphoma kinase; C – classical; CD – cluster of differentiation; CK – (pan) cytokretin; EGFR – epidermal growth factor receptor; EML4 – echinoderm microtubule-associated protein-like 4; ETV6 – ETS variant transcription factor 6; F – female; IFP – inflammatory fibroid polyp; IMT – inflammatory myofibroblastic tumor; IHC – immunohistochemistry; M – male; NTRK – neurotrophic tyrosine receptor kinase; PPARGC1A – peroxisome proliferator-activated receptor gamma, coactivator 1 alpha; RANBP – RAN-binding protein; SMA – smooth muscle actin; vim – vimentin.

variant of IMT. Case 4 was characterized by a translocation involving the *NTRK3* and *ETV6* genes. In case 5, an *EGFR-PPARGC1A* rearrangement, which was deemed nonfunctional due to the absence of a promoter, was identified in a gastric inflammatory fibroid polyp (Table 2).

Gene variants

Eighty-four genetic changes, including substitutions, insertions, duplications, and deletions, were identified across 58 gene variants through RNA NGS analysis. According to the Varsome database (https://varsome.com), these variants were classified as follows: 15 pathogenic, 17 likely pathogenic, 38 of uncertain significance, and 14 benign (Table 3). The most frequently observed pathogenic variants were nucleotide substitutions at positions 34 and 35 of the *KRAS* gene. These mutations were detected in multiple cases, including EIMS (case 3), Langerhans cell histiocytosis (case 11), inflammatory fibroid polyp (case 16), and IPTs (cases 21, 24 and 27).

Additionally, the most commonly identified likely pathogenic variant involved a cytosine-to-thymine substitution at position 2975 of the *MET* gene. The mutation was

Table 3. List of gene variants detected using of NGS and their significance according to the Varsome database (https://varsome.com/)

Case number	Diagnosis (fusion gene)	Gene	HGVSp	HGVSc	VAF	Gene variant significance	Recurrence
1	IMT (*EML4-ALK*)	MET	p.Asn375Ser	c.1124A>G	0.663	benign	1 year
		RET	p.Val25Ala	c.74T>C	0.051	benign	
		RET	p.Leu27Ser	c.80T>C	0.050	uncertain	
2	IMT (*EML4-ALK*)	none	–	–	–	–	no
3	EIMS (*RANBP2-ALK*)	EGFR	p.Gln276Ter	c.826C>T	0.090	uncertain	no
		KRAS	p.Gly12Cys	c.34G>T	0.067	pathogenic	
		NTRK3	p.Leu449Phe	c.1345C>T	0.051	uncertain	
4	IMT (*ETV6-NTRK3*)	none	–	–	–	–	no
5	inflammatory fibroid polyp (*EGFR-PPARGC1A*)	none	–	–	–	–	no
6	granular cell tumor	FGFR3	p.Val642_ Leu645delinsIleHisHisIle	c.1924_1933delinsATTCACCACA	0.956	uncertain	6 years
7	plasma cell myeloma	BRAF	p.Gly315AspfsTer57	c.944del	0.564	likely pathogenic	no
		EGFR	p.Glu746Val	c.2237A>T	0.071	uncertain	
		EGFR	p.Leu747_ Pro753delinsSer	c.2240_2257del	0.067	pathogenic	
		RET	p.Leu27Ser	c.80T>C	0.052	uncertain	
8	fibroma	FGFR3	p.Val642_ Leu645delinsIleHisHisIle	c.1924_1933delinsATTCACCACA	0.897	uncertain	no
		EGFR	p.Ser768Ile	c.2303G>T	0.569	pathogenic	
		MET	p.Thr992Ile	c.2975C>T	0.552	likely pathogenic	
		EGFR	p.Gly719Ala	c.2156G>C	0.529	pathogenic	
9	anaplastic meningioma	none	–	–	–	–	4 months
10	submucosal fibromatosis	none	–	–	–	–	no
11	Langerhans cell histiocytosis	KRAS	p.Gly12Val	c.35G>T	0.065	pathogenic	no
		ALK	p.Met1199Ile	c.3597G>A	0.063	uncertain	no
12	desmoid fibromatosis	ALK	p.Met1199Ile	c.3597G>A	0.058	uncertain	1st: 1 year, 2nd: 6 years
		RET	p.Leu27Ser	c.80T>C	0.051	uncertain	
13	sarcomatoid urothelial carcinoma	EGFR	p.His870Tyr	c.2608C>T	0.063	uncertain	1st: 1 month, 2nd: 2 months
14	plexiform fibromyxoma	BRAF	p.Lys591Glu	c.1771A>G	0.065	pathogenic	no
15	angiosarcoma	FGFR3	p.Val642_ Leu645delinsIleHisHisIle	c.1924_1933delinsATTCACCACA	1.0	uncertain	no
16	inflammatory fibroid polyp	KRAS	p.Gly12Cys	c.34G>T	0.981	pathogenic	no
		BRAF	p.Ile572Val	c.1714A>G	0.167	uncertain	
		ALK	p.Thr1026Pro	c.3076A>C	0.119	benign	
		BRAF	p.Arg603Ter	c.1807C>T	0.081	likely pathogenic	
17	inflammatory fibroid polyp	BRAF	p.Arg603Ter	c.1807C>T	0.556	likely pathogenic	no
		BRAF	p.Arg444Gln	c.1331G>A	0.357	uncertain	
		BRAF	p.Ser446_ Ser447delinsLeuAsn	c.1337_1340delinsTGAA	0.294	uncertain	
		ALK	p.Thr1026Pro	c.3076A>C	0.105	benign	
18	inflammatory fibroid polyp	MET	p.Thr992Ile	c.2975C>T	0.889	likely pathogenic	no

Table 3. List of gene variants detected using of NGS and their significance according to the Varsome database (https://varsome.com/) – cont.

Case number	Diagnosis (fusion gene)	Gene	HGVSp	HGVSc	VAF	Gene variant significance	Recurrence
19	GIST	MET	p.Thr992Ile	c.2975C>T	0.060	likely pathogenic	2 years
20	neurofibroma	BRAF	p.Asn581Tyr	c.1741A>T	0.579	pathogenic	no
21	IPT	KRAS	p.Gly12Cys	c.34G>T	0.331	pathogenic	no
		EGFR	p.Gln1020Ter	c.3058C>T	0.082	uncertain	
		NTRK3	p.Pro514Leu	c.1541C>T	0.054	likely pathogenic	
22	IPT	BRAF	p.Gly469Ala	c.1406G>C	0.438	pathogenic	no
		NTRK2	p.Pro50Leu	c.149C>T	0.063	uncertain	no
		FGFR3	p.Arg124Trp	c.370C>T	0.051	uncertain	no
23	IPT (associated with small cell carcinoma)	FGFR1	p.Pro151Ser	c.451C>T	0.056	likely pathogenic	no
24	IPT	KRAS	p.Gly12Val	c.35G>T	0.402	pathogenic	no
		FGFR3	p.Val364TrpfsTer30	c.1090del	0.192	likely pathogenic	
		MET	p.His1079Tyr	c.3235C>T	0.188	uncertain	
25	IPT	ROS1	P.Ser1891LysfsTer18	c.5671dup	0.054	uncertain	no
26	IPT	BRAF	p.Gly315AspfsTer57	c.944del	0.406	likely pathogenic	no
		RET	p.Leu27Ser	c.80T>C	0.068	uncertain	
27	infective IPT	KRAS	p.Gly12Ala	c.35G>C	0.248	pathogenic	no
		BRAF	p.Ser446_ Ser447delinsLeuAsn	c.1337_1340delinsTGAA	0.192	uncertain	
		BRAF	p.Arg603Ter	c.1807C>T	0.208	likely pathogenic	
		BRAF	p.Arg444Gln	c.1331G>A	0.179	uncertain	
		FGFR1	p.Thr724Ile	c.2171C>T	0.077	likely pathogenic	
28	IPT – dacryoadenitis	BRAF	p.Asn581Tyr	c.1741A>T	0.579	pathogenic	no
29	IPT	BRAF	p.Ile617Phe	c.1848_1849delinsTT	0.714	uncertain	no
		BRAF	p.Arg603Ter	c.1807C>T	0.24	likely pathogenic	
		BRAF	p.Trp619Cys	c.1857G>T	0.083	pathogenic	
30	infective IPT	RET	p.Arg886Trp	c.2656C>T	0.549	uncertain	no
		MET	p.Thr992Ile	c.2975C>T	0.469	likely pathogenic	
31	infective IPT	FGFR1	p.Gln762Ter	c.2284C>T	0.1	uncertain	1 year
32	IPT	BRAF	p.Pro367Leu	c.1100C>T	0.140	uncertain	no
		NTRK1	p.Thr434Met	c.1301C>T	0.109	benign	
		EGFR	p.Gln40Ter	c.118C>T	0.078	uncertain	
		BRAF	p.Pro301Leu	c.902C>T	0.059	benign	
33	IPT	ALK	p.Thr1026Pro	c.3076A>C	0.086	benign	no
		BRAF	p.Arg603Ter	c.1807C>T	0.076	likely pathogenic	
		ALK	p.His1030Pro	c.3089A>C	0.065	benign	
		BRAF	p.His539Tyr	c.1615C>T	0.058	uncertain	
		BRAF	p.Glu533Ter	c.1597G>T	0.057	uncertain	
		BRAF	p.Phe583Val	c.1747T>G	0.057	uncertain	
		BRAF	p.Phe548Ser	c.1643T>C	0.056	uncertain	
		BRAF	p.Lys591Glu	c.1770_1771delinsGG	0.05	likely pathogenic	

Table 3. List of gene variants detected using of NGS and their significance according to the Varsome database (https://varsome.com/) – cont.

Case number	Diagnosis (fusion gene)	Gene	HGVSp	HGVSc	VAF	Gene variant significance	Recurrence
34	IPT	NTRK3	p.Val308Met	c.922G>A	0.559	benign	no
		EGFR	p.Ser229Cys	c.685A>T	0.095	uncertain	
35	IPT – aneurysm wall	ALK	p.Thr1026Pro	c.3076A>C	0.333	benign	no
		ALK	p.His1030Pro	c.3089A>C	0.079	benign	
36	xanthogranulomatous pyelonephritis	BRAF	p.Gly32_Ala33dup	c.95_100dup	0.431	benign	no
		ALK	p.Thr1026Pro	c.3076A>C	0.145	benign	
37	infective IPT	BRAF	p.Ala349del	c.1046_1048del	0.051	uncertain	no
38	ischemic fasciitis (associated with mammary carcinoma)	MET	p.Thr992Ile	c.2975C>T	0.06	likely pathogenic	no
39	IPT	FGFR1	p.Ala411Val	c.1232C>T	0.152	uncertain	no
		KRAS	p.Ser39Phe	c.116C>T	0.096	uncertain	
		FGFR1	p.Arg716Cys	c.2146C>T	0.078	pathogenic	
		EGFR	p.Phe44Ser	c.131T>C	0.073	benign	
		KRAS	p.Gln43Ter	c.127C>T	0.056	uncertain	
40	IPT (associated with colon adenocarcinoma)	FGFR3	p.Ser779Asn	c.2336G>A	0.06	uncertain	no
41	spindle cell SCC	none	–	–	–	–	6 months
42	solitary fibrous tumor	none	–	–	–	–	no
43	leiomyoma	none	–	–	–	–	1 month
44	IPT (after treatment of DLBCL)	none	–	–	–	–	no
45	IPT – sinusitis	none	–	–	–	–	no
46	IMT/PMP	NGS not performed				–	1 month

ALK – anaplastic lymphoma kinase; BRAF – B-type rapidly accelerated fibrosarcoma; DLBCL – diffuse large B-cell lymphoma; EGFR – epidermal growth factor receptor; EIMS – epithelioid inflammatory myofibroblastic sarcoma; FGFR – fibroblast growth factor receptor; GIST – gastrointestinal stromal tumor; HGVSc – Human Genome Variation Society coding sequence name; HGVSp – Human Genome Variation Society protein sequence name; IMT – inflammatory myofibroblastic tumor; IPT – inflammatory pseudotumor; KRAS – Kirsten rat sarcoma; MET – mesenchymal-to-epithelial transition factor; NGS – next-generation sequencing; NTRK – neurotrophic tyrosine receptor kinase; PMP – pseudosarcomatous myfibroblastic proliferation; RET – rearranged during transfection; ROS1 – v-ras avian UR2 sarcoma virus oncogene homolog 1; SCC – squamous cell carcinoma; VAF – variant allele frequency.

found in several cases, including orbital fibroma (case 8), inflammatory fibroid polyp (case 18), gastrointestinal stromal tumor (GIST – case 19), infective IPT (case 30), and ischemic fasciitis (case 38). Substitutions at position 1807 of the *BRAF* gene were also detected in inflammatory fibroid polyps (cases 16 and 17) and IPTs (cases 27, 29 and 33).

Clonality

The NGS gene panel revealed clonality in a majority of the neoplasms studied. At least 1 gene variant with a VAF value greater than 0.5 or a functional gene rearrangement was identified in 50% of the neoplasms. Lower values of VAF and no functional rearrangement were found in 29% of patients. Only 21% of examined neoplasms did not present either mutation or rearrangement. Moreover, genetic alterations were identified in 82% of inflammatory lesions, cases with VAF values exceeding 0.5 in 18% of inflammatory lesions and with a VAF range of 0–0.5 in 64%. The OR for the presence of at least 1 functional rearrangement or genetic alteration with a VAF of 0.5 or higher in the neoplastic group compared to the reactive group was approx. 5.85. This result was statistically significant at the 95% confidence level (95% CI: 1.50–22.83, p = 0.011), calculated using the method described by Tenny et al.[25]

Clinical follow-up

The maximum observation for the study was 17 years. During this time, 10 patients (21.7%) died within a maximum of 6 years following the surgery. The causes of deaths were related to severe neoplastic diseases, including plasma cell myeloma (case 7), anaplastic meningioma (case 9), desmoid fibromatosis (case 12), angiosarcoma (case 15), and

Table 4. Collective description of histological features of recurrent lesions during the study

Case number	Location	Final diagnosis	Pattern	Ganglion-like cells	Atypia	Necrosis	Mitotic activity	Inflammatory infiltrate intensity	Dominating inflammatory cells	Recurrence	Period of observation	Death
1	external nose	IMT	C	(–)	mild	10%	(–)	severe	histiocytes	1 year	7 years	no
6	right frontal sinus	granular cell tumor	C	(–)	none	none	(–)	severe	lymphocytic	6 years	13 years	no
9	right occipital region	anaplastic meningioma	mixed	(+)	severe	40%	20/10 HPF	mild	lymphocytic	4 months	1 year 4 months	yes
12	right axillary region	desmoid fibromatosis	C	(+)	moderate	40%	1/10 HPF	moderate	histiocytes	1st:1 year, 2nd: 6 years	6 years	yes
13	urinary bladder	sarcomatoid urothelial carcinoma	C	(+)	severe	10%	19/10 HPF	mild	mixed	1st: 1 month, 2nd: 2 months	7 years	no
19	small intestine	GIST	↑	(–)	mild	3%	1/10 HPF	mild	lymphocytic	2 years	2 years	yes
31	left orbit	infective IPT	C	(–)	mild	10%	(–)	severe	mixed	6 months	2 years	yes
41	larynx	spindle cell squamous cell carcinoma	mixed	(–)	severe	10%	6/10 HPF	moderate	neutrophils	6 months	1 year	no
43	mesentery	leiomyoma	↑/C	(–)	none	none	(–)	moderate	lymphocytic	1 month	2 years	no
46	urinary bladder	IMT/PMP	C	(–)	mild	40%	1/10 HPF	mild	neutrophils	1 month	12 years	no

↑ – hypocellular; (–) – absent; C – classical; IMT – inflammatory myofibroblastic tumor; IPT – inflammatory pseudotumor; HPF – high-power fields; PMP – pseudosarcomatous myofibroblastic proliferation.

intestinal GIST (case 19). One patient (case 35) died post-surgery due to an abdominal aortic rupture. The overall odds of death were 0.33 in the neoplastic group and 0.22 in the reactive group.

During the surveillance period, which ranged from 1 to 13 years, 10 patients (21.7%) experienced local recurrence of their disease (Table 4). Nine of these cases were neoplastic in origin, including IMT (case 1), granular cell tumor (case 6), anaplastic meningioma (case 9), desmoid fibromatosis (case 12), sarcomatoid urothelial carcinoma (case 13), intestinal GIST (case 19), spindle cell squamous cell carcinoma (case 41), leiomyoma (case 43), and IMT/pseudosarcomatous myfibroblastic proliferation (PMP) (case 46). Episodes of double recurrence were observed in desmoid fibromatosis (case 12) and sarcomatoid urothelial carcinoma (case 13). One reactive lesion, classified as infective IPT (case 31), also presented a recurrence. The overall odds of recurrence were 0.6 in the neoplastic group and 0.048 in the reactive group. The OR for recurrence (12.6) was statistically significant at the 95% confidence level (95% CI: 1.44–10.32, p = 0.022), calculated based on method described by Tenny et al.[25] Four patients died following local recurrence, including those with anaplastic meningioma (case 9), desmoid-type fibromatosis (case 12), intestinal GIST (case 19), and infective IPT (case 31).

Patients diagnosed with IMTs survived until the end of the study with observation periods lasting between 1 and 8 years. Recurrence was noted in only 1 IMT with the *EML4-ALK* fusion gene (case 1), occurring 1 year after the initial surgery. No distant metastases were observed during the follow-up period.

Clinicopathological relation

Histopathological features and local recurrence

Ganglion-like cells were identified in specimens from 3 patients with recurrent neoplastic tumors (Table 4), including anaplastic meningioma of the right occipital region (case 9), desmoid fibromatosis of the right axillary region (case 12) and sarcomatoid urothelial carcinoma of the urinary bladder (case 13) (Fig. 6).

The OR for the presence of nuclear atypia in the group with recurrent disease compared to the non-recurrent group was 12, which was statistically significant at the 5% level (95% CI: 2.14–67.24, p = 0.005), calculated using the method described by Tenny et al.[25] This suggests that nuclear atypia is associated with an adverse prognosis and an increased risk of disease recurrence. Four cases showed severe nuclear atypia (Table 4). Three of them, anaplastic meningioma of the right occipital region (case 9), sarcomatoid urothelial carcinoma of the urinary bladder (case 13) and spindle cell squamous cell carcinoma of the larynx (case 41), presented recurrence. One patient with angiosarcoma of the ileum (case 15) died within 3 days after the operation. Desmoid fibromatosis (case 12) presented moderate atypia and recurred twice.

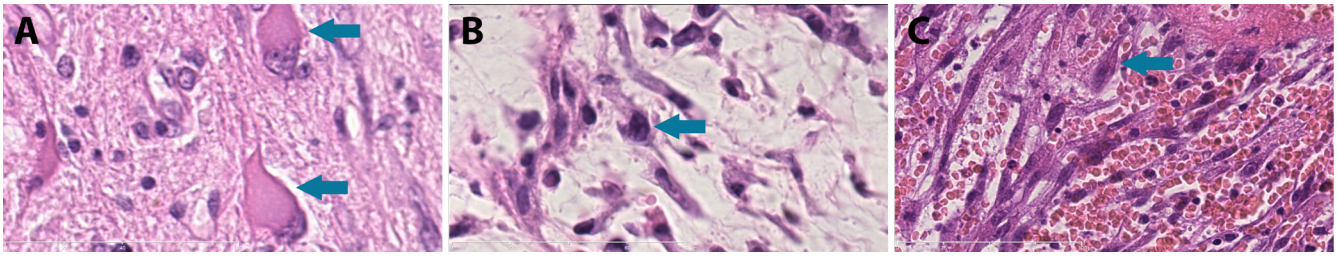

Fig. 6. Ganglion-like cells (blue arrows) – hematoxylin and eosin (H&E) staining. A. Anaplastic meningioma of the right occipital region (case 9), ×1000 magnification; B. Desmoid fibromatosis of the right axillary region (case 12), ×1000 magnification; C. Sarcomatoid urothelial carcinoma of the urinary bladder (case 13), ×630 magnification

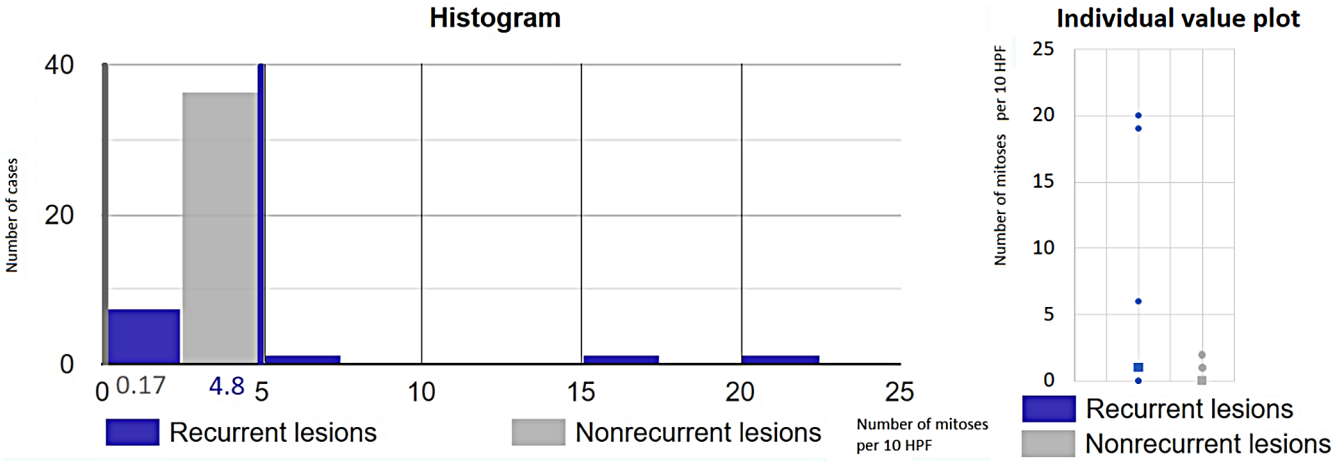

Fig. 7. Histogram (left) depicts the distribution of mitoses among recurrent (blue) and non-recurrent lesions (grey). The arithmetic mean values are marked with vertical lines. Axes: abscissa – intervals of mitotic index values in the histopathological slides: [0/10HPF–5/10HPF), [5/10HPF–10/10HPF), [10/10HPF–15/10HPF), [15/10HPF–20/10HPF), and [20/10HPF–25/10HPF]; ordinate – number of cases. Individual value plot (right) shows a dot for the actual value of each observation in both groups. The median values are marked with squares. Axes: abscissa – group of cases (blue: recurrent, grey: non-recurrent); ordinate – mitotic index values

HPF – high-power fields.

An increased mitotic rate (>5 mitoses per 10 high-power fields) was observed in 3 recurrent cases: anaplastic meningioma (case 9), sarcomatoid urothelial carcinoma (case 13) and spindle cell squamous cell carcinoma (case 41). Recurrence occurred in all 3 cases within 6 months (Table 4). Statistical analysis using the Mann–Whitney U test (U = 269, p = 0.002) revealed a significant difference in mitotic index values between recurrent lesions (mean: 4.8/10 HPF) and non-recurrent lesions (mean: 0.17/10 HPF), confirming statistical significance at the 5% level (Fig. 7).

Although no statistically significant relationship was found between necrosis and recurrence, the necrosis percentage differed significantly between patients who died during the study and patients who survived. It was assessed using the Mann–Whitney U test (U = 253, p = 0.043), which showed a statistically significant difference between 1st (arithmetic mean: 22.3%) and 2nd group (arithmetic mean: 12.14%) at the 95% CI (Fig. 8).

Genetic alterations and local recurrence

Disease recurrence was observed in 6 patients with identified genetic alterations (Tables 2,3). One IMT (case 1) harbored a fusion gene *EML4-ALK* and benign or uncertain mutations in the *MET* and *RET* genes. However, recurrences were not observed in case with other fusion genes. A recurrence was noted in intestinal *GIST* (case 19), which presented a likely pathogenic substitution in the *MET* gene. Four additional cases with genetic alterations of uncertain significance also experienced relapses. Notably, desmoid fibromatosis (case 12) and sarcomatoid urothelial carcinoma (case 13), both with genes of unknown significance, exhibited double recurrence during the follow-up period.

Diagnosis correctness verification

Following final diagnosis verification, patients were categorized into neoplastic and inflammatory groups (Table 5). Diagnostic accuracy for neoplasms was highly satisfactory with a sensitivity of 0.708, specificity of 0.818, accuracy of 0.761, precision of 0.81, and an F1 score of 0.756. Neoplastic lesions were subsequently classified into specific nosological entities. However, diagnostic performance for IMT was significantly lower with a sensitivity of 0.6, specificity of 0.537, accuracy of 0.543, precision of 0.136, and an F1 score 0.222 (Table 6, Fig. 9).

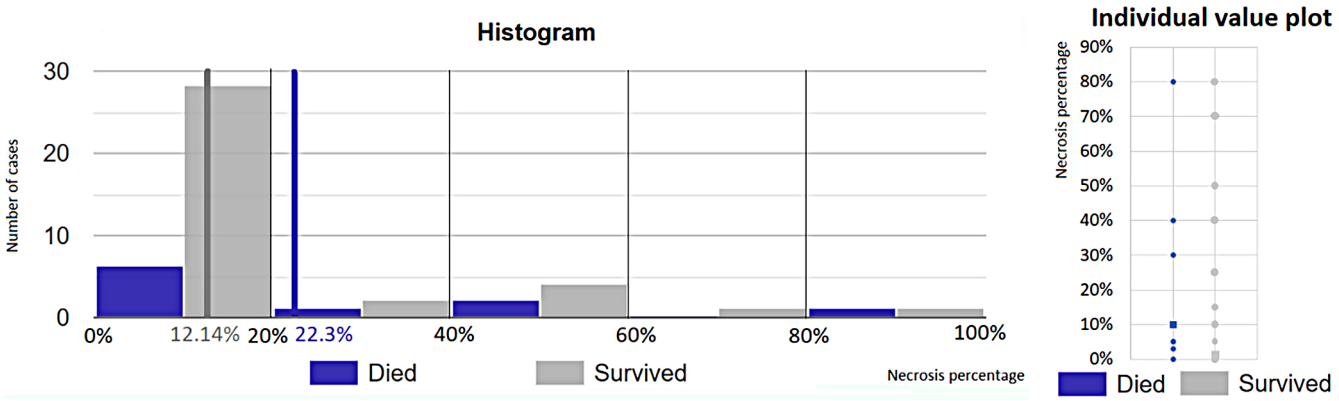

Fig. 8. Histogram (left) depicts the distribution of necrosis among patients who died (blue) and survived (grey) in the analyzed period. The arithmetic mean values are marked with vertical lines. Axes: abscissa – necrosis percentage intervals in the histopathological slides: [0%–20%), [20%–40%), [40%–60%), [60%–80%), and [80%–100%]; ordinate – number of cases. Individual value plot (right) shows a dot for the actual value of each observation in both groups. The median values are marked with squares. Axes: abscissa – groups of patients (blue: who died, grey: who survived); ordinate – necrosis percentage

Table 5. Quantity of diagnosed entities

Neoplastic lesions	Number
Inflammatory myofibroblastic tumor	5
Inflammatory fibroid polyp	4
Leiomyoma	1
Plexiform fibromyxoma	1
Gastrointestinal stromal tumor	1
Desmoid fibromatosis	1
Solitary fibrous tumor	1
Fibroma	1
Angiosarcoma	1
Neurofibroma	1
Anaplastic meningioma	1
Submucosal fibrosis	1
Sarcomatoid urothelial carcinoma	1
Spindle cell squamous cell carcinoma	1
Granular cell tumor	1
Langerhans cell histiocytosis	1
Plasma cell myeloma	1
Reactive lesions	
IPT, not otherwise specified	12
Infective IPT	4
IPT associated with a neoplasm	2
IPT – wall of aneurysm	1
Xanthogranulomatous pyelonephritis	1
Chronic dacryoadenitis	1
Ischemic fasciitis	1

IPT – inflammatory pseudotumor.

Discussion

Inflammatory spindle cell lesions appear to represent an artificial and heterogeneous group of entities, and the term is rarely used in contemporary literature. Many distinct diseases can be differentiated from within this category.[1,2,26–28] Establishing an accurate diagnosis is extremely challenging and requires clinicopathological correlation, genetic testing and considerable time, as also demonstrated by the findings of this study. Moreover, making a definitive diagnosis without ancillary tests is nearly impossible, as noted in previous reports.[13,19,29,30] Unfortunately, such diagnostic tools are typically available only in highly specialized medical centers. Therefore, the term "inflammatory spindle cell lesion" may be appropriately used in pathology departments with limited diagnostic resources, where molecular techniques are unavailable. However, the final diagnosis should ideally be confirmed in specialized soft tissue pathology centers using molecular assays.

Entities from the ISCL group are a rare occurrence, making it difficult to collect a sufficient number of cases to standardize research protocols.[20] In this study, we aimed to gather as many tumors as possible and successfully included 46 cases. Inflammatory myofibroblastic tumor (IMT) remains the most representative entity within the ISCL spectrum,[1] which is why our focus was placed on investigating tyrosine kinase gene rearrangements. The final diagnosis of IMT requires a typical histopathological image and the presence of certain fusions. Detection of tyrosine kinase gene fusions using FISH, PCR or NGS plays a crucial role in confirming the diagnosis and assessing the prognosis of IMT.[20,31] However, only NGS can provide comprehensive information about novel fusion genes.[32–34]

Interestingly, our cohort was predominantly composed of middle-aged and older adults, which contrasts with the typical age distribution reported for IMT in the existing literature.[20] As the population ages, the prevalence of certain diseases increases, some of which can be severe and contribute to higher mortality. In older populations, comparing local recurrence rates is more relevant, as recurrence appears to be influenced by the final pathological diagnosis, anatomical location and type of surgical resection. Literature supports an association between these factors and local recurrence.[35]

Table 6. Confusion matrices of diagnosis correctness verification

Diagnosis correctness verification					
Neoplasm vs other diseases			IMT vs other diseases		
Predicted condition	actual condition		Predicted condition	Actual condition	
Total population (n = 46)	positive (n = 24)	negative (n = 22)	total population (n = 46)	positive (n = 5)	negative (n = 41)
Positive (n = 21)	TP (n = 17)	FP (n = 4)	positive (n = 22)	TP (n = 3)	FP (n = 19)
Negative (n = 25)	FN (n = 7)	TN (n = 18)	negative (n = 24)	FN (n = 2)	TN (n = 22)

FN – false negative; FP – false positive; IMT – inflammatory myofibroblastic tumor; TN – true negative; TP – true positive.

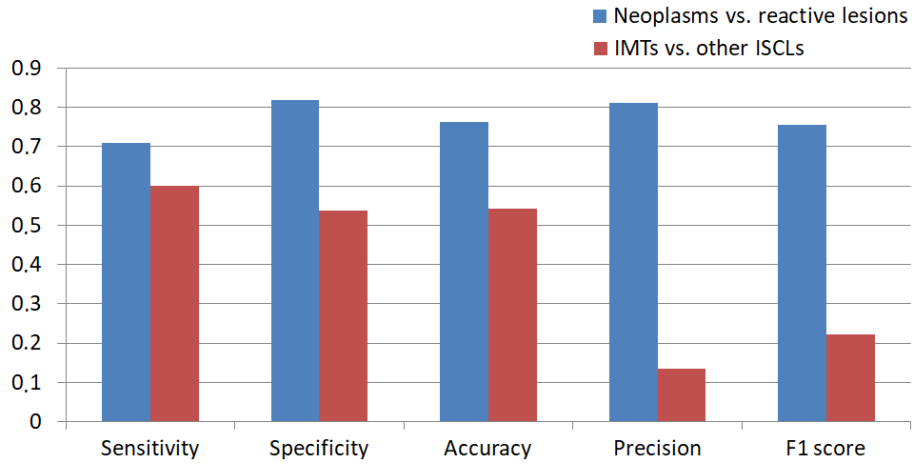

Fig. 9. Column chart presents the diagnosis correctness values of neoplastic lesion (blue) and inflammatory myofibroblastic tumor (IMT; red)

In this study, primary histopathological diagnoses were compared to final diagnoses, which were based on clinical and paraclinical data. The results indicate that histopathological diagnostics are highly satisfactory for distinguishing between neoplastic and reactive lesions. However, primary recognition of IMT was inconsistent with the final diagnosis. The low values of precision, F1 score and sensitivity highlight the risk of diagnostic inaccuracies, even within academic medical centers. This aligns with prior publications highlighting the risk of misdiagnosis in histopathological evaluation of ISCLs.[10,36–41] Our findings underline the prevalence of this problem.

In IMT histopathological slides, the presence of intercellular mucus, ganglion-like cells, giant cells, necrosis, increased mitotic activity, and high cellularity are considered adverse prognostic factors.[3,42] In this study, local recurrences were observed in other neoplastic ISCLs containing ganglion-like cells, nuclear atypia and increased mitotic activity (Table 4). Statistical analysis revealed that the OR of these histological features significantly separated neoplastic from reactive groups within a 95% CI. Although no association was found between tissue pattern, necrosis or inflammatory infiltrate intensity and local recurrence as prognostic factors, a higher estimated necrosis percentage was observed in patients who died compared to those who survived with the difference being statistically significant. Thus, the presence of ganglion-like cells, nuclear atypia, increased mitotic activity, and necrosis should be noted in pathological reports as negative prognostic factors.

No relationship between genetic changes and clinical outcomes was identified (Tables 2,3). Consistent with the literature, *ALK* gene fusions were the most frequent,[20] present in 75% of IMTs confirmed with sequencing in this study (Table 2). Only 1 neoplasm (case 4) exhibited an *NTRK3*-rearrangement and *EML4-ALK* fusion genes were detected in 2 IMTs (cases 1 and 2). This fusion gene has also been identified in anaplastic large cell lymphoma, as well as colorectal and breast cancers.[43] It contributes to tumorigenesis by producing a transcript that includes the intracellular kinase domain of ALK and the trimerization domain of EML4, enabling constitutive ALK activation through oligomerization and autophosphorylation. Tumors harboring this fusion are generally responsive to treatment with tyrosine kinase inhibitors.[44]

RANBP1-ALK, *RANBP2-ALK* and *RRBP1-ALK* rearrangements are characteristic of EIMS, a malignant IMT variant with an aggressive clinical course.[31,45] These fusions produce distinctive nuclear membrane or perinuclear accentuation patterns in ALK immunohistochemical staining.[45] In case 3, the *RANBP2-ALK* gene was associated with focal nuclear membranous ALK positivity. Complete surgical removal of the neoplasm resulted in no recurrence over a 7-year follow-up period.

The *ETV6* gene, a member of the ETS transcription factor family, regulates gene expression by nuclear binding. *NTRK* genes encode tropomyosin receptor kinases, which are crucial for neuronal tissue development and functioning.[17,28] The *ETV6-NTRK3* fusion gene has been detected in several neoplasms, including ALK-negative

IMT, congenital infantile fibrosarcoma, acute myeloblastic leukemia, secretory breast carcinoma, mammary analog secretory carcinoma of the salivary gland, papillary thyroid carcinoma, and congenital mesoblastic nephroma.[46] Differentiation between IMT and congenital infantile fibrosarcoma can be challenging, as both tumors may exhibit similar behavior. Histopathological features, such as classical pattern, inflammatory infiltrate and patients age above 1 year suggest an IMT rather than congenital infantile fibrosarcoma.[47] Both tumors may also respond to tyrosine kinase inhibitors, underscoring the overlap in their management. Histologically, the term "inflammatory fibrosarcoma" has even been used synonymously with IMT.[30]

In the urinary bladder, pseudosarcomatous myofibroblastic proliferations (PMPs) typically present grossly as nodular or polypoid ulcerative masses and exhibit microscopic features that closely resemble those of classical IMTs.[48] Pseudosarcomatous myofibroblastic proliferations occur mainly in slightly older populations, are more cellular, and have shorter cells and fewer plasma cells than IMTs. While PMP tends to follow a slightly more aggressive course, both lesions can exhibit *ALK* fusions. However, the *ALK* breakpoint differs, being situated in exons 18 or 19 for PMP and exon 20 for IMT.[9] In this study, differentiation between the 2 entities in case 46 was not possible due to low-quality RNA in the FFPE block. The histopathological findings and ALK-positivity in immunohistochemical assays were consistent with both entities (Fig. 10). Treatment for PMP and IMT is similar,[20,48] and some authors consider them synonymous.[49]

Case 5 was ultimately diagnosed as a gastric inflammatory fibroid polyp containing the *EGFR-PPARGC1A* fusion gene. This rearrangement has previously been reported only in chronic sun exposure-related cutaneous squamous cell carcinoma.[50] In this case, the fusion appeared to be nonfunctional due to the absence of the *EGFR* gene promoter kinase domain (exon 20).[51] In certain IMTs, the coexistence of an *EML4-ALK* rearrangement and an activating *EGFR* mutation plays a significant role in resistance to tyrosine kinase inhibitors.[44] Since the *EGFR* gene is located on the short arm of chromosome 7 and the *PPARGC1A* gene on the short arm of chromosome 4, this fusion may result from a chromosomal translocation.

Indeed, IPT is thought to be a reactive lesion,[1] but it can recur after surgical resection, especially when an incomplete excision is performed.[51,52] Moreover, if a causative agent persists in the organism, the recurrence may take place, as a result of ineffective antibiotic therapy in infections or insufficient suppressive treatment in autoimmune diseases. Such a situation was also observed in this study (case 31). However, the OR of relapse in our neoplastic compared to reactive group is approx. 12.6 and statistically significant within the 95% CI, which suggests local relapse tends to be more common for neoplasms.

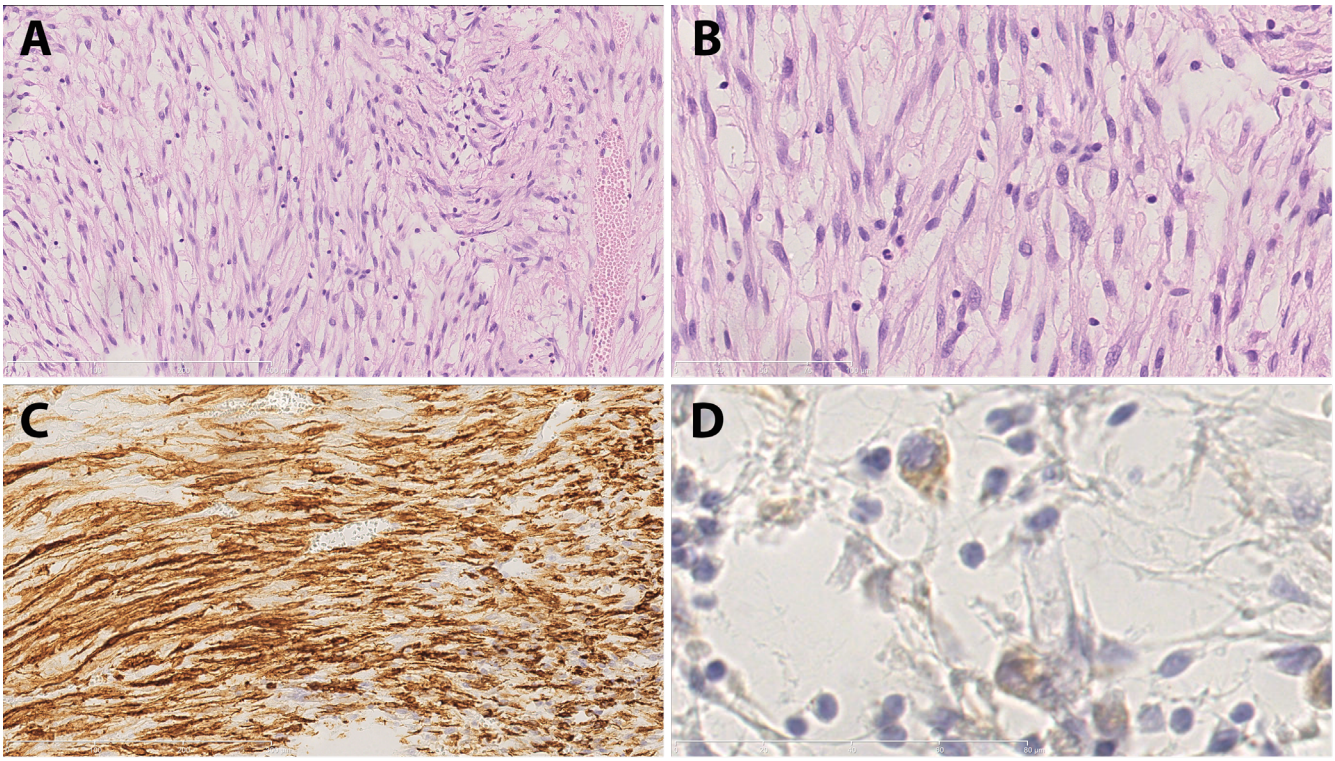

Fig. 10. Case 46. A. Hematoxylin and eosin (H&E) staining, ×200 magnification; B. H&E staining, ×400 magnification; C. Immunohistochemical staining against smooth muscle actin, ×200 magnification; D. Immunohistochemical staining against anaplastic lymphoma kinase (ALK), ×1000 magnification

In this study, neoplasms exhibited features such as ganglion-like cells, atypical cells and mitoses more frequently than reactive lesions. Ganglion-like cells, according to the literature, may occur in benign,[53] intermediate and malignant neoplasms,[54] but are also found in reactive lesions like proliferative myositis and necrotizing fasciitis.[55] The presence of nuclear atypia is typically associated with a worse prognosis and is more commonly found in neoplastic lesions.[56] In the neoplastic group, the presence of mitoses is associated with worse outcomes. Also, atypical mitotic figures can be found in neoplasms.[57] Reactive lesions can also contain multiple mitoses, but are never atypical.[58]

Necrosis, calcifications and extravasated erythrocytes are rare in IMTs.[59] Höhne et al. noted the presence of necrosis both in IMTs and IPTs but did not define a differentiating percentage.[60] In this study, IMTs showed a significantly higher necrosis percentage than other ISCLs, as confirmed using the Mann–Whitney U test. Furthermore, a higher necrosis percentage was statistically associated with increased mortality.

Certain benign non-neoplastic lesions with histopathological features, like hypercellularity, cytological atypia and increased mitotic activity, are classified as psuedosarcomas.[61] Integrating clinical and paraclinical data can help avoid misdiagnosing inflammatory lesions as sarcomas.

Interestingly, mutations were also observed in reactive lesions. While genetic clonality is a hallmark of neoplasms,[47] clonal expansion is possible in non-cancerous lesions. The presence of driver mutations in these tissues may indicate an early tumorigenesis, which does not always progress to neoplasm development.[62] Factors like aging, chronic inflammation and environmental exposures support clonal expansion.[62,63] Neoplasm development and progression require the accumulation of genetic mutations and epigenetic alterations, so a single change may not be sufficient to induce a real tumorigenesis.[63] In this study, 82% of inflammatory lesions exhibited genetic clonality, which is consistent with this theory. The number of functional fusion genes with frequencies above 50% and variants with VAF values greater than 0.5 distinguished neoplastic from reactive lesions using the Mann–Whitney U test.

Limitations

This study has several limitations: 1) all cases were diagnosed within a single pathology department, potentially limiting generalizability; 2) only cases initially diagnosed as IMT or IPT were included, which may have introduced selection bias; 3) it was not possible to retrieve all FFPE blocks and histological slides; and 4) a limited targeted NGS gene panel was used. Detailed comparisons are provided in Supplementary Table 1.

Conclusions

This study underscores the importance of integrating clinical and paraclinical data to achieve an accurate diagnosis. Prognosis is influenced more significantly by the final pathological diagnosis, anatomical location of the lesion and completeness of surgical resection than by isolated histopathological or genetic findings. However, neoplastic etiology and some of the features, such as the presence of ganglion-like cells, nuclear atypia and increased mitotic activity, can occur in lesions that present local recurrences. The study strongly supports the theory, which assumes that not only neoplasms but also reactive diseases can present worrisome histological features, pathogenic mutations and genetic clonality. However, neoplastic ISCLs more frequently exhibited ganglion-like cells, nuclear atypia, elevated mitotic index, and the presence of functional gene rearrangements or point mutations with a VAF ≥ 0.5 compared to reactive lesions. Notably, both lesion types may recur if the underlying causative factor persists following excision. Among the detected functional gene rearrangements, the most frequent involved ALK and *NTRK3* genes, which are considered key drivers in inflammatory myofibroblastic tumors.

Confirmation of tyrosine receptor kinase gene rearrangements is necessary for diagnosing IMTs, which showed a higher necrosis percentage than other ISCLs. A higher necrosis percentage was also linked to increased mortality. In summary, this study confirms the prognostic significance of a neoplastic diagnosis, presence of ganglion-like cells, nuclear atypia, elevated mitotic index, and increased necrosis percentage. It also highlights the diagnostic value of ganglion-like cells, nuclear atypia, higher mitotic activity, and functional gene rearrangements or point mutations with a VAF ≥ 0.5. These features should be consistently reported in pathology assessments to support informed clinical decision-making.

Supplementary data

The supplementary materials are available at https://doi.org/10.5281/zenodo.15034538. The package includes the following files:

Supplementary Table 1. Full dataset of the study.

Data availability

The datasets generated and/or analyzed during the current study are available from the corresponding author on reasonable request.

Consent for publication

Not applicable.

Use of AI and AI-assisted technologies

Not applicable.

ORCID iDs

Krzysztof Siemion https://orcid.org/0000-0003-2354-9891
Joanna Kiśluk https://orcid.org/0000-0002-1668-0288
Natalia Wasilewska https://orcid.org/0000-0001-6327-8526
Joanna Reszec-Gielażyn https://orcid.org/0000-0002-0169-0897
Anna Korzyńska https://orcid.org/0000-0002-6488-4832
Tomasz Łysoń https://orcid.org/0000-0002-9757-8276
Zenon Mariak https://orcid.org/0000-0003-4132-9278

References

1. Kutok JL, Pinkus GS, Dorfman DM, Fletcher CDM. Inflammatory pseudotumor of lymph node and spleen: An entity biologically distinct from inflammatory myofibroblastic tumor. *Hum Pathol*. 2001;32(12):1382–1387. doi:10.1053/hupa.2001.29679
2. Irani S, Rabbani Anari M, Yazdani Bioki F, Nasirmohtaram S, Kaedi Z, Alipour S. Inflammatory myofibroblastic tumor: Two cases in head and neck region. *Indian J Otolaryngol Head Neck Surg*. 2022;74(Suppl 3):6394–6399. doi:10.1007/s12070-022-03119-9
3. Siemion K, Reszec-Gielazyn J, Kisluk J, Roszkowiak L, Zak J, Korzynska A. What do we know about inflammatory myofibroblastic tumors? A systematic review. *Adv Med Sci*. 2022;67(1):129–138. doi:10.1016/j.advms.2022.02.002
4. Chávez-Peón Berle E, Hallman C, Kleinhenz K, Plattner BL. Multifocal spinal inflammatory myofibroblastic tumors in a juvenile paraparetic dog. *Vet Radiol Ultrasound*. 2023;64(2):E14–E18. doi:10.1111/vru.13195
5. Moro A, De Angelis P, Gasparini G, et al. Orbital desmoid-type fibromatosis: A case report and literature review. *Case Rep Oncol Med*. 2018;2018:1684763. doi:10.1155/2018/1684763
6. Hu G, Chen H, Liu Q, et al. Plexiform fibromyxoma of the stomach: A clinicopathological study of 10 cases. *Int J Clin Exp Pathol*. 2017;10(11):10926–10933. PMID:31966436. PMCID:PMC6965819.
7. Kai K, Miyosh A, Aishima S, et al. Granulomatous reaction in hepatic inflammatory angiomyolipoma after chemoembolization and spontaneous rupture. *World J Gastroenterol*. 2015;21(32):9675–9682. doi:10.3748/wjg.v21.i32.9675
8. Hornick JL, Sholl LM, Dal Cin P, Childress MA, Lovly CM. Expression of ROS1 predicts *ROS1* gene rearrangement in inflammatory myofibroblastic tumors. *Modern Pathol*. 2015;28(5):732–739. doi:10.1038/modpathol.2014.165
9. Acosta AM, Demicco EG, Dal Cin P, Hirsch MS, Fletcher CDM, Jo VY. Pseudosarcomatous myofibroblastic proliferations of the urinary bladder are neoplasms characterized by recurrent FN1–ALK fusions. *Modern Pathol*. 2021;34(2):469–477. doi:10.1038/s41379-020-00670-0
10. Völker HU, Scheich M, Höller S, et al. Differential diagnosis of laryngeal spindle cell carcinoma and inflammatory myofibroblastic tumor: Report of two cases with similar morphology. *Diagn Pathol*. 2007;2:1. doi:10.1186/1746-1596-2-1
11. Lopez-Beltran A, Montironi R, Raspollini MR, Cheng L, Netto GJ. Iatrogenic pathology of the urinary bladder. *Semin Diagn Pathol*. 2018;35(4):218–227. doi:10.1053/j.semdp.2018.03.001
12. Arslan ME, Li H, Fu Z, Jennings TA, Lee H. Plexiform fibromyxoma: Review of rare mesenchymal gastric neoplasm and its differential diagnosis. *World J Gastrointest Oncol*. 2021;13(5):409–423. doi:10.4251/wjgo.v13.i5.409
13. Croce S, Hostein I, McCluggage WG. *NTRK* and other recently described kinase fusion positive uterine sarcomas: A review of a group of rare neoplasms. *Genes Chromosomes Cancer*. 2021;60(3):147–159. doi:10.1002/gcc.22910
14. Tariq MU, Din NU, Abdul-Ghafar J, Park YK. The many faces of solitary fibrous tumor: Diversity of histological features, differential diagnosis and role of molecular studies and surrogate markers in avoiding misdiagnosis and predicting the behavior. *Diagn Pathol*. 2021;16(1):32. doi:10.1186/s13000-021-01095-2
15. Zhang BX, Chen ZH, Liu Y, Zeng YJ, Li YC. Inflammatory pseudotumor-like follicular dendritic cell sarcoma: A brief report of two cases. *World J Gastrointest Oncol*. 2019;11(12):1231–1239. doi:10.4251/wjgo.v11.i12.1231
16. Khatri A, Agrawal A, Sikachi R, Mehta D, Sahni S, Meena N. Inflammatory myofibroblastic tumor of the lung. *Adv Respir Med*. 2018;86(1):27–35. doi:10.5603/ARM.2018.0007
17. Antonescu CR. Emerging soft tissue tumors with kinase fusions: An overview of the recent literature with an emphasis on diagnostic criteria. *Genes Chromosomes Cancer*. 2020;59(8):437–444. doi:10.1002/gcc.22846
18. Dall Bello AG, Severo CB, Guazzelli LS, Oliveira FM, Hochhegger B, Severo LC. Histoplasmosis mimicking primary lung cancer or pulmonary metastases. *J Bras Pneumol*. 2013;39(1):63–68. doi:10.1590/S1806-37132013000100009
19. Armstrong V, Khazeni K, Rosenberg A, Swain SK, Moller M. Inflammatory pseudotumor secondary to urachal cyst: A challenging clinical case report. *Int J Surg Case Rep*. 2020;66:360–364. doi:10.1016/j.ijscr.2019.12.029
20. Gros L, Dei Tos AP, Jones RL, Digklia A. Inflammatory myofibroblastic tumour: State of the art. *Cancers (Basel)*. 2022;14(15):3662. doi:10.3390/cancers14153662
21. Coffin CM, Hornick JL, Fletcher CDM. Inflammatory myofibroblastic tumor: Comparison of clinicopathologic, histologic, and immunohistochemical features including ALK expression in atypical and aggressive cases. *Am J Surg Pathol*. 2007;31(4):509–520. doi:10.1097/01.pas.0000213393.57322.c7
22. Weir MM, Rosenberg AE, Bell DA. Grading of spindle cell sarcomas in fine-needle aspiration biopsy specimens. *Am J Clin Pathol*. 1999;112(6):784–790. doi:10.1093/ajcp/112.6.784
23. Klintrup K, Mäkinen JM, Kauppila S, et al. Inflammation and prognosis in colorectal cancer. *Eur J Cancer*. 2005;41(17):2645–2654. doi:10.1016/j.ejca.2005.07.017
24. World Health Organization (WHO). Soft Tissue and Bone Tumours. 5th ed. Geneva, Switzerland: World Health Organization (WHO); 2020. ISBN: 978-92-832-4502-5, 978-92-832-4503-2.
25. Tenny S, Hoffman MR. Odds ratio. In: *StatPearls*. Treasure Island, USA: StatPearls Publishing; 2025:Bookshelf ID: NBK431098. http://www.ncbi.nlm.nih.gov/books/NBK431098. Accessed March 19, 2025.
26. Shah A, Pey E, Achonu JU, Bai JDK, Khan F. Inflammatory myofibroblastic tumor 12 years after treatment for synovial sarcoma: A case report. *Orthop Res Rev*. 2021;13:163–169. doi:10.2147/ORR.S333124
27. Hisaoka M, Shimajiri S, Matsuki Y, et al. Inflammatory myofibroblastic tumor with predominant anaplastic lymphoma kinase-positive cells lacking a myofibroblastic phenotype. *Pathol Int*. 2003;53(6):376–381. doi:10.1046/j.1440-1827.2003.01484.x
28. Yamamoto H, Nozaki Y, Kohashi K, Kinoshita I, Oda Y. Diagnostic utility of pan-Trk immunohistochemistry for inflammatory myofibroblastic tumours. *Histopathology*. 2020;76(5):774–778. doi:10.1111/his.14010
29. Tauziède-Espariat A, Duchesne M, Baud J, et al. *NTRK*-rearranged spindle cell neoplasms are ubiquitous tumours of myofibroblastic lineage with a distinct methylation class. *Histopathology*. 2023;82(4):596–607. doi:10.1111/his.14842
30. Al Shenawi H, Al-Shaibani SA, Al Saad SK, et al. An extremely rare case of malignant jejunal mesenteric inflammatory myofibroblastic tumor in a 61-year-old male patient: A case report and literature review. *Front Med (Lausanne)*. 2022;9:1042262. doi:10.3389/fmed.2022.1042262
31. Giannaki A, Doganis D, Giamarelou P, Konidari A. Epithelioid inflammatory myofibroblastic sarcoma presenting as gastrointestinal bleed: Case report and literature review. *JPGN Rep*. 2021;2(1):e019. doi:10.1097/PG9.0000000000000019
32. Antonescu CR, Suurmeijer AJH, Zhang L, et al. Molecular characterization of inflammatory myofibroblastic tumors with frequent *ALK* and *ROS1* gene fusions and rare novel RET rearrangement. *Am J Surg Pathol*. 2015;39(7):957–967. doi:10.1097/PAS.0000000000000404
33. Strom SP. Current practices and guidelines for clinical next-generation sequencing oncology testing. *Cancer Biol Med*. 2016;13(1):3–11. doi:10.28092/j.issn.2095-3941.2016.0004
34. Drilon A, Jenkins C, Iyer S, Schoenfeld A, Keddy C, Davare MA. ROS1-dependent cancers: Biology, diagnostics and therapeutics. *Nat Rev Clin Oncol*. 2021;18(1):35–55. doi:10.1038/s41571-020-0408-9
35. Cantin J, McNeer GP, Chu FC, Booher RJ. The problem of local recurrence after treatment of soft tissue sarcoma. *Ann Surg*. 1968;168(1):47–53. doi:10.1097/00000658-196807000-00005

36. Agaimy A, Märkl B. Inflammatory angiomyolipoma of the liver: An unusual case suggesting relationship to IgG4-related pseudotumor. *Int J Clin Exp Pathol*. 2013;6(4):771–779. PMID:23573326. PMCID:PMC3606869.
37. Taylor MS, Chougule A, MacLeay AR, et al. Morphologic overlap between inflammatory myofibroblastic tumor and IgG4-related disease: Lessons from next-generation sequencing. *Am J Surg Pathol*. 2019;43(3):314–324. doi:10.1097/PAS.0000000000001167
38. Tran TAN, Chang KTE, Kuick CH, Goh JY, Chang CC. Local ALK-positive histiocytosis with unusual morphology and novel *TRIM33-ALK* gene fusion. *Int J Surg Pathol*. 2021;29(5):543–549. doi:10.1177/1066896920976862
39. Lee J, Singh A, Ali SM, Lin DI, Klempner SJ. TNS1-ALK fusion in a recurrent, metastatic uterine mesenchymal tumor originally diagnosed as leiomyosarcoma. *Acta Med Acad*. 2019;48(1):116. doi:10.5644/ama2006-124.248
40. Carballo EV, Pham TV, Turashvili G, Hanley K, Starbuck KD, Meisel JL. Recurrent uterine inflammatory myofibroblastic tumor previously managed as leiomyosarcoma has sustained response to alectinib. *Gynecol Oncol Rep*. 2022;43:101062. doi:10.1016/j.gore.2022.101062
41. Kojima M, Nakamura S, Ohno Y, Sugihara S, Sakata N, Masawa N. Hepatic angiomyolipoma resembling an inflammatory pseudotumor of the liver: A case report. *Pathol Res Pract*. 2004;200(10):713–716. doi:10.1016/j.prp.2004.08.001
42. Choi M, Kim W, Cheon MG, Lee CW, Kim JE. Polo-like kinase 1 inhibitor BI2536 causes mitotic catastrophe following activation of the spindle assembly checkpoint in non-small cell lung cancer cells. *Cancer Lett*. 2015;357(2):591–601. doi:10.1016/j.canlet.2014.12.023
43. Roskoski R. Anaplastic lymphoma kinase (ALK): Structure, oncogenic activation, and pharmacological inhibition. *Pharmacol Res*. 2013;68(1):68–94. doi:10.1016/j.phrs.2012.11.007
44. Hunt AL, Nutcharoen A, Randall J, et al. Integration of multi-omic data in a molecular tumor board reveals EGFR-associated ALK-inhibitor resistance in a patient with inflammatory myofibroblastic cancer. *Oncologist*. 2023;28(8):730–736. doi:10.1093/oncolo/oyad129
45. Lee JC, Li CF, Huang HY, et al. ALK oncoproteins in atypical inflammatory myofibroblastic tumours: Novel RRBP1-ALK fusions in epithelioid inflammatory myofibroblastic sarcoma. *J Pathol*. 2017;241(3):316–323. doi:10.1002/path.4836
46. Takahashi A, Kurosawa M, Uemura M, Kitazawa J, Hayashi Y. Anaplastic lymphoma kinase-negative uterine inflammatory myofibroblastic tumor containing the *ETV6-NTRK3* fusion gene: A case report. *J Int Med Res*. 2018;46(8):3498–3503. doi:10.1177/0300060518780873
47. Lindberg MR, ed. *Diagnostic Pathology: Soft Tissue Tumors*. 3rd ed. Philadelphia, USA: Elsevier; 2019. ISBN:978-0-323-71149-4.
48. Harik LR, Merino C, Coindre JM, Amin MB, Pedeutour F, Weiss SW. Pseudosarcomatous myofibroblastic proliferations of the bladder: A clinicopathologic study of 42 cases. *Am J Surg Pathol*. 2006;30(7):787–794. doi:10.1097/01.pas.0000208903.46354.6f
49. Tanaka T, Ueda T, Yokoyama T, Harada S, Hatakeyama K, Yoshimura A. Pseudosarcomatous myofibroblastic proliferation of the appendix with an abdominal abscess due to diverticulum perforation: A case report. *Surg Case Rep*. 2020;6(1):144. doi:10.1186/s40792-020-00901-1
50. Egashira S, Jinnin M, Ajino M, et al. Chronic sun exposure-related fusion oncogenes *EGFR-PPARGC1A* in cutaneous squamous cell carcinoma. *Sci Rep*. 2017;7(1):12654. doi:10.1038/s41598-017-12836-z
51. Wang F, Li C, Wu Q, Lu H. EGFR exon 20 insertion mutations in non-small cell lung cancer. *Transl Cancer Res*. 2020;9(4):2982–2991. doi:10.21037/tcr.2020.03.10
52. Goto T, Akanabe K, Maeshima A, Kato R. Surgery for recurrent inflammatory pseudotumor of the lung. *World J Surg Oncol*. 2011;9(1):133. doi:10.1186/1477-7819-9-133
53. Coffin CM, Alaggio R. Fibroblastic and myofibroblastic tumors in children and adolescents. *Pediatr Dev Pathol*. 2012;15(1 Suppl):127–180. doi:10.2350/10-12-0944-PB.1
54. Barak S, Wang Z, Miettinen M. Immunoreactivity for calretinin and keratins in desmoid fibromatosis and other myofibroblastic tumors: A diagnostic pitfall. *Am J Surg Pathol*. 2012;36(9):1404–1409. doi:10.1097/PAS.0b013e3182556def
55. Domanski HA, Qian X, Åkerman M, Stanley DE. Soft tissue. In: Domanski HA, ed. *Atlas of Fine Needle Aspiration Cytology*. Cham, Switzerland: Springer International Publishing; 2019:465–551. doi:10.1007/978-3-319-76980-6_14
56. Hunis AP, Hunis M. Soft tissue sarcomas. *J Inter Med Emer Res*. 2022;3(3):1–51. doi:10.37191/Mapsci-2582-7367-3(3)-049
57. Kallen ME, Hornick JL. The 2020 WHO classification: What's new in soft tissue tumor pathology? *Am J Surg Pathol*. 2021;45(1):e1–e23. doi:10.1097/PAS.0000000000001552
58. Gobbi H, Tse G, Page DL, Olson SJ, Jensen RA, Simpson JF. Reactive spindle cell nodules of the breast after core biopsy or fine-needle aspiration. *Am J Surg Pathol*. 2000;113(2):288–294. doi:10.1309/RPW4-CXCC-1JHM-0TL7
59. Surabhi VR, Chua S, Patel RP, Takahashi N, Lalwani N, Prasad SR. Inflammatory myofibroblastic tumors. *Radiol Clin North Am*. 2016;54(3):553–563. doi:10.1016/j.rcl.2015.12.005
60. Höhne S, Milzsch M, Adams J, Kunze C, Finke R. Inflammatory pseudotumor (IPT) and inflammatory myofibroblastic tumor (IMT): A representative literature review occasioned by a rare IMT of the transverse colon in a 9-year-old child. *Tumori J*. 2015;101(3):249–256. doi:10.5301/tj.5000353
61. Rosenberg AE. Pseudosarcomas of soft tissue. *Arch Pathol Lab Med*. 2008;132(4):579–586. doi:10.5858/2008-132-579-POST
62. Kakiuchi N, Ogawa S. Clonal expansion in non-cancer tissues. *Nat Rev Cancer*. 2021;21(4):239–256. doi:10.1038/s41568-021-00335-3
63. Hibino S, Kawazoe T, Kasahara H, et al. Inflammation-induced tumorigenesis and metastasis. *Int J Mol Sci*. 2021;22(11):5421. doi:10.3390/ijms22115421